Conference paper
UDC 535.34
DOI: https://doi.org/10.18721/JPM.191.102

Electric field-induced anisotropy of absorption and refraction of terahertz radiation in *n*-InSb

R.V. Ustimenko, V.A. Shalygin, D.A. Karaulov, I.A. Norvatov, G.A. Melentev, M.Ya. Vinnichenko ✉, D.A. Firsov

Peter the Great St. Petersburg Polytechnic University, St. Petersburg, Russia
✉ mvin@spbstu.ru

Abstract. The effect of an electric field on the optical characteristics of bulk *n*-InSb in the terahertz spectral range (wavelength of 119 μm) at a temperature of 78 K was experimentally studied. The observed changes in the absorption coefficient and refractive index are explained by an increase in the average energy of electrons in an electric field, which is accompanied by a change in the average inverse effective mass of electrons due to the non-parabolicity of the conduction band. Along with the isotropic change in the optical characteristics in electric field, a dependence of the absorption and refraction of terahertz radiation on the direction of the polarization vector was revealed: the measurement results are different for electromagnetic radiation linearly polarized parallel and perpendicular to the field. A comparison of the experimental results with the results of theoretical modeling showed that the observed anisotropy of absorption and refraction is associated with the combined action of two factors: the non-parabolicity of the conduction band and the anisotropy of the nonequilibrium distribution function of electrons over states in momentum space.

Keywords: distribution function anisotropy, electron heating, electron drift, radiation absorption, radiation refraction, polarization of radiation, InSb

Funding: The reported study was funded by Russian Science Foundation (Grant No. 23-12-00036), https://rscf.ru/project/23-12-00036/.

For citation: Ustimenko R.V., Shalygin V.A., Karaulov D.A., Norvatov I.A., Melentev G.A., Vinnichenko M.Ya., Firsov D.A., Electric field-induced anisotropy of absorption and refraction of terahertz radiation in *n*-InSb, St. Petersburg State Polytechnical University Journal. Physics and Mathematics. 19 (1.1) (2026) 12–20. DOI: https://doi.org/10.18721/JPM.191.102

Конференционная статья
УДК 535.34
DOI: https://doi.org/10.18721/JPM.191.102

Индуцированная электрическим полем анизотропия поглощения и преломления терагерцового излучения в *n*-InSb

Р.В. Устименко, В.А. Шалыгин, Д.А. Караулов, И.А. Норватов, Г.А. Мелентьев, М.Я. Винниченко ✉, Д.А. Фирсов

Санкт-Петербургский политехнический университет Петра Великого, Санкт-Петербург, Россия
✉ mvin@spbstu.ru

Аннотация. Экспериментально исследовано влияние электрического поля на оптические характеристики объемного *n*-InSb в терагерцовом спектральном диапазоне (длина волны 119 мкм) при температуре 78 K. Обнаруженные изменения коэффициента поглощения и показателя преломления объясняются увеличением средней энергии электронов в электрическом поле, что сопровождается

изменением средней обратной эффективной массы электронов вследствие непараболичности зоны проводимости. Наряду с изотропным изменением оптических характеристик в электрическом поле обнаружена зависимость поглощения и преломления терагерцового излучения от направления вектора поляризации: параллельно или перпендикулярно полю. Сравнение результатов эксперимента с результатами теоретического моделирования показало, что обнаруженная анизотропия поглощения и преломления связана с совместным действием двух факторов: непараболичности зоны проводимости и анизотропии неравновесной функции распределения электронов по состояниям в импульсном пространстве.

Ключевые слова: анизотропия функции распределения, разогрев электронов, дрейф электронов, поглощение излучения, преломление излучения, поляризация излучения, InSb

Финансирование: Работа выполнена при финансовой поддержке Российского научного фонда (грант № 23-12-00036), https://rscf.ru/project/23-12-00036/.

Для цитирования: Устименко Р.В., Шалыгин В.А., Караулов Д.А., Норватов И.А., Мелентьев Г.А., Винниченко М.Я., Фирсов Д.А. Индуцированная электрическим полем анизотропия поглощения и преломления терагерцового излучения в *n*-InSb // Научно-технические ведомости СПбГПУ. Физико-математические науки. 2026. Т. 19. № 1.1. С. 12–20. DOI: https://doi.org/10.18721/JPM.191.102

Introduction

Electro-optical effects are widely used to modulate electromagnetic radiation. Due to the rapid development of terahertz (THz) optoelectronics and photonics, the study of electro-optical effects in this spectral region is of great current interest [1, 2]. The aim of this work is to experimentally investigate the anisotropy of THz radiation absorption and refraction that occurs in an optically isotropic semiconductor when exposed to an electric field.

The object of our study is donor-doped indium antimonide single crystals. The experiment directly measures the modulation of the sample's optical transmission when exposed to electric field pulses. The microscopic mechanism of the observed modulation can be associated with a field-induced change in the free electron contribution to the permittivity of *n*-InSb. The peculiarity of indium antimonide is that this semiconductor has a non-parabolic conduction band. The effect of an electric field in this case is accompanied by a change in the dielectric constant, which is different for radiation with linear polarization along the field (extraordinary wave) and perpendicular to it (ordinary wave). Previously, such an effect was experimentally observed in *n*-InSb in the mid-IR range ($\lambda = 10.6$ μm) [3]. In the cited work, the wavelength was significantly shorter than the wavelengths of the plasmon-phonon resonance, the absorption of radiation by free electrons was negligible, and the effect was entirely reduced to a change in the refractive index, which was different for ordinary and extraordinary waves.

In this work, experiments were conducted in the THz range. The radiation wavelength ($\lambda \approx 119$ μm) is an order of magnitude longer than in [3] and is close to the wavelength of the low-frequency plasmon-phonon mode in the samples studied. In this case, the situation is more complex: there is noticeable absorption by free electrons, and the modulation of the sample transmission by the electric field is associated with two factors, namely, a change in the refractive index and a change in the absorption coefficient. Moreover, the change in the absorption coefficient also turns out to be different for ordinary and extraordinary waves. Theoretical modeling of the electric field-induced anisotropy of absorption and refraction of terahertz radiation in *n*-InSb was previously performed in [4].

The aim of this work is to obtain experimental data on the field dependence of the refractive index and absorption coefficient, as well as their polarization anisotropy in the THz spectral range for indium antimonide. For this purpose, an original research method was developed and tested, based on parallel measurements of the electro-optical modulation of laser radiation under

conditions of multipath interference and in its absence. The obtained experimental data were compared with model calculations.

Experimental technique

All samples were fabricated from the same *n*-InSb single crystal with a free electron concentration of $N_e = 3.5 \cdot 10^{15}$ cm^{-3} and a low-field mobility of $\mu(0) = 1.2 \cdot 10^5$ cm^2/(V·s) (at a temperature of $T_0 = 78$ K). The samples were dumbbell-shaped (see the inset in Fig. 1, *a*). First, plane disks of about a millimeter thickness were cut from the single crystal using an electrical discharge machine. The disks were subjected to mechanical grinding and polishing, as a result of which the thickness was reduced to 0.6–0.7 mm. Then, dumbbells were cut from the polished disks, also using an electrical discharge machine. The dumbbell shape of the samples helps to create a uniform electric field in the working region and reduces the current density through the contacts.

In the neck of a dumbbell with a small cross-section $w \times d$ and length $L >> w, d$, a uniform electric field was created by applying a pulsed voltage V to the contacts of the sample. The contact regions of the sample were 6 – 7 times wider than the width of the dumbbell neck w, and their length was 4 – 5 times shorter than L. Therefore, the resistance of the contact regions was negligible, and the electric field strength E in the dumbbell neck can be calculated using the formula $E = V / L$. Ohmic contacts on the ends of the sample were created by electrolytic deposition of nickel from a Ni_2SO_4 solution.

A continuous gas laser with optical pumping by CO_2 laser radiation, namely, a methanol vapor laser FIRL-100 (Edinburgh Instruments) with an operating wavelength of $\lambda = 118.8$ μm, was used as a source of THz radiation. The laser beam was focused onto the polished face of the dumbbell neck using an off-axis parabolic mirror, and the beam aperture was limited by a diaphragm. The beam path length in the sample was equal to d. Switching of radiation polarization from the **e** ∥ **E** state to the **e** ⊥ **E** state was carried out using a half-wave quartz plate (here **e** and **E** denote the unit polarization vector and vector of applied electric field, respectively). The sample was mounted in a flooded nitrogen cryostat with TPX windows and had a temperature of $T_0 = 78$ K. The radiation transmitted through the sample was focused using two parabolic mirrors onto a Ge:Ga detector (QMC Instruments), cooled to 4.2 K in a closed-cycle cryostat. Photoresponse signals were measured with a TDS 2014B oscilloscope (Tektronix).

In the first series of samples (samples PP), the polished surfaces were plane-parallel (the deviation from plane-parallelism did not exceed 1 μm within the laser beam probing region). Multiple reflections of the laser beam from the input and output surfaces of the sample were

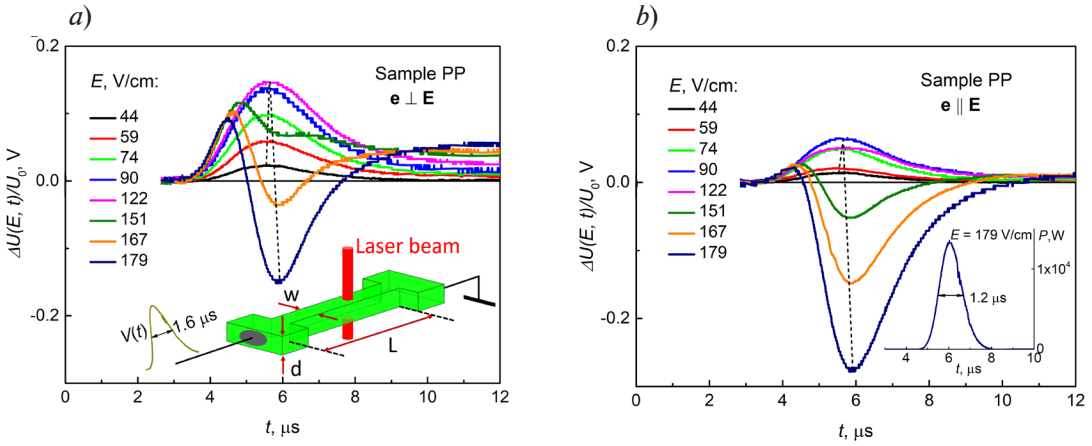

Fig. 1. Transmission modulation in sample PP with pulsed electric field (experiment): oscillograms of photoresponse signal pulse $\Delta U(E, t)$ for an ordinary wave (**e** ⊥ **E**), (*a*), and an extraordinary wave (**e** ∥ **E**), (*b*), normalized to the amplitude of the periodic photoresponse signal at the chopper frequency U_0.
In the legend, *E* denotes the amplitude of the electric field pulse.
Inset to (*a*): sample configuration for the electrooptical measurements, *V*(*t*) shows shape of the voltage pulse.
Inset to (*b*): power pulse shape

accompanied by multipath Fabry–Pérot interference. The optical transmittance of the sample in this case is described by the Airy formula:

$$T = \frac{(1-r)^2 e^{-\alpha d}}{1 - 2re^{-\alpha d}\cos(\delta) + r^2 e^{-2\alpha d}}, \quad (1)$$

where

$$r = \frac{(1-n)^2 + k^2}{(1+n)^2 + k^2}, \quad (2)$$

is the intensity reflection coefficient of the *n*-InSb/vacuum interface under normal incidence of a beam of monochromatic electromagnetic radiation, $\alpha = 4\pi k/\lambda$ is the absorption coefficient, *n* and *k* denote the refractive index and extinction coefficient of the *n*-InSb, respectively, and $\delta = 4\pi nd/\lambda$ is the interference phase (the phase shift during double passage of radiation through the sample). When the electric field E varied in the range of 0–180 V/cm, the interference phase changed significantly, which made a noticeable contribution to the modulation of the sample's transmission, along with the field-induced change in the absorption coefficient.

In the second series of samples (samples C), the output surface of the dumbbell neck had a *cylindrical* shape, with its thickness being greatest at the center and gradually decreasing toward its edges. This surface shape was achieved by additional grinding and polishing of the dumbbell neck. As a result, the interference phase δ took on different values at different points of the probing laser spot, and Fabry–Pérot interference was suppressed. In this case, the optical transmittance of the sample can be described by the formula:

$$T = \frac{(1-r)^2 e^{-\alpha d}}{1 - r^2 e^{-2\alpha d}}. \quad (3)$$

The geometric dimensions of the two samples, the experimental data for which are presented in this paper, are given in Table.

Table

Dimensions of the samples

Sample	*L*, mm	*w*, mm	*d*, mm
Sample PP	10	0.8	0.613
Sample C	16	1.2	0.699

The laser beam was modulated by a chopper at a frequency of 160 Hz. Bell-shaped electric field pulses of 1.6 μs duration (see inset in Fig. 1, *a*) were synchronized with the chopper and had a frequency 80 times lower, ensuring negligible Joule heating of the sample's crystal lattice when exposed to periodic pulses. Experiments were conducted in pre-breakdown electric fields ($E \leq 180$ V/cm), where the free electron concentration remains constant.

The magnitude of the field-induced modulation of the sample transmission *M* was determined as follows:

$$M(E) = \frac{T(E) - T(0)}{T(0)}, \quad (4)$$

where $T(E)$ denotes the transmittance of the sample in the field *E*.

Results and discussion

The oscillograms of the photoresponse signal pulses in sample PP (Fig. 1) and sample C (Fig. 2) differ qualitatively. In sample C, for both radiation polarizations (**e** ∥ **E** and **e** ⊥ **E**), the photoresponse signal remains positive over the entire range of the studied electric fields, which corresponds to a field-induced increase in the sample transmittance. Sample PP exhibits bipolar photoresponse signals in strong fields: when the supplied electric power approaches the peak value, the photoresponse signal becomes negative, indicating a decrease in the sample transmittance. In Fig. 1 and 2, the time dependences of the photoresponse signal $\Delta U(E, t)$, induced by the electric field, are normalized to the amplitude U_0 of the periodic photoresponse signal at the chopper frequency.

Note that the pulse of supplied electric power had a duration of 1.2 μs (see inset in Fig. 1, *b*) and with increasing field the pulse peak shifted by +0.2 μs. The photodetector had a time constant

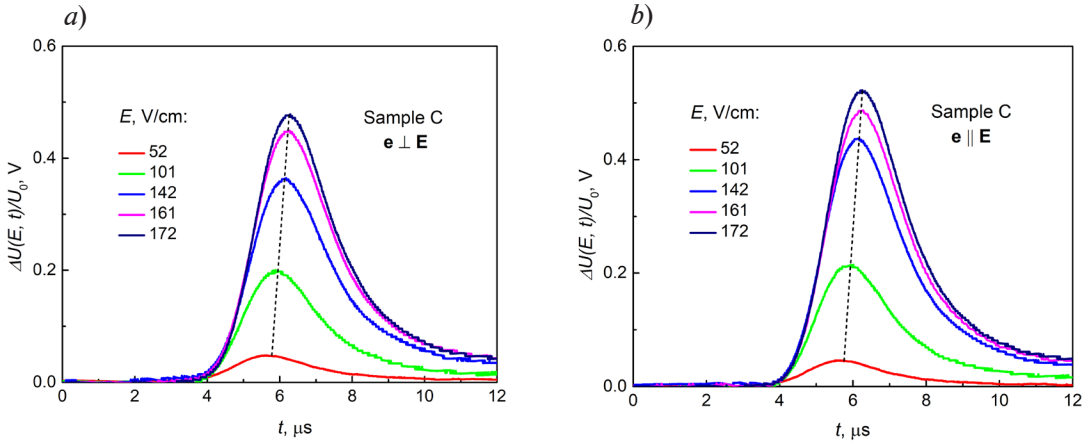

Fig. 2. Modulation of sample transmission with electric field pulses (experiment): oscillograms of photoresponse signal pulse for an ordinary wave (*a*) and an extraordinary wave (*b*), normalized to the amplitude of the periodic photoresponse signal at the chopper frequency

of ~1.3 μs, while the photoresponse pulse duration was ~2.5 μs, and with increasing field its peak shifted by +0.4 μs. In Fig. 1 and 2, the shift of the photoresponse signal peak is shown by dashed lines. In each oscillogram, the dashed line indicates the value of the ratio $\Delta U(E, t)/U_0$, which coincides with the modulation value $M(E)$, defined by Eq. (4).

The experimental field dependences of the transmission modulation for both samples are shown in Fig. 3. Their joint analysis allows us to determine the electric field-induced changes in the absorption coefficient and refractive index for the single crystal from which the samples are made.

As noted in the previous section, in sample C the Fabry–Pérot interference is suppressed, and its transmittance can be described by Eq. (3). Then, in the approximation $r \approx \text{const}(E)$ (which is satisfied with an accuracy of 1% for the sample under study), the field-induced change in the absorption coefficient can be found from the value of M using the equation:

$$\Delta\alpha(E) = -\frac{1}{d}\ln\left[M(E)+1\right], \tag{5}$$

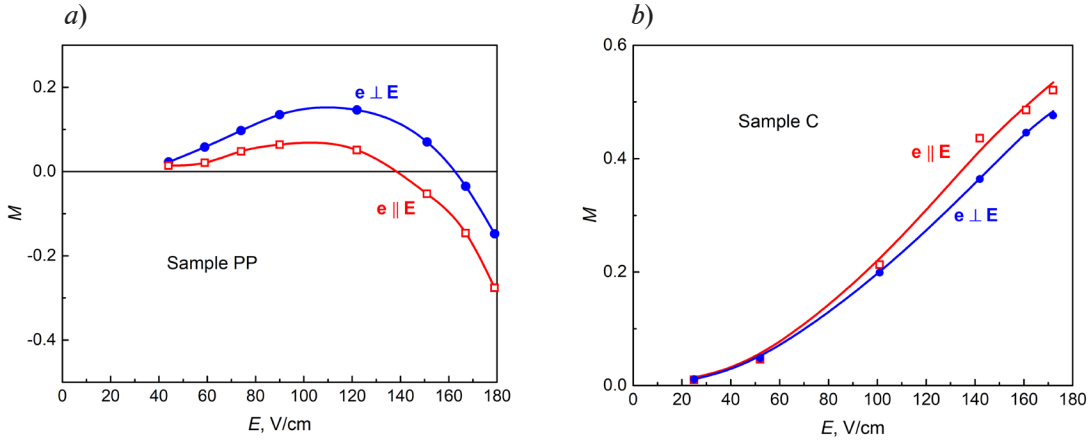

Fig. 3. Experimental field dependences of transmission modulation for ordinary (circles) and extraordinary (squares) waves: sample PP (*a*), sample C (*b*).
Solid lines are a guide for the eye

The resulting field dependences of the electric-field-induced change in the absorption coefficient of *n*-InSb, $\Delta\alpha_P(E)$, for radiation of two mutually orthogonal linear polarizations (P = ⊥, ∥) are shown in Fig. 4, *a*. Note that for both polarizations the electric field induces negative changes in transmission, and at a given field $|\Delta\alpha_{\parallel}(E)| > |\Delta\alpha_{\perp}(E)|$. In the maximum field (172 V/cm), the average change in the absorption coefficient $[\Delta\alpha_{\parallel}(E) + \Delta\alpha_{\perp}(E)]/2$ reaches a value of -6 cm^{-1}, and the polarization anisotropy reaches a value of $|\alpha_{\parallel}(E) - \Delta\alpha_{\perp}(E)| = 0.45$ cm^{-1}.

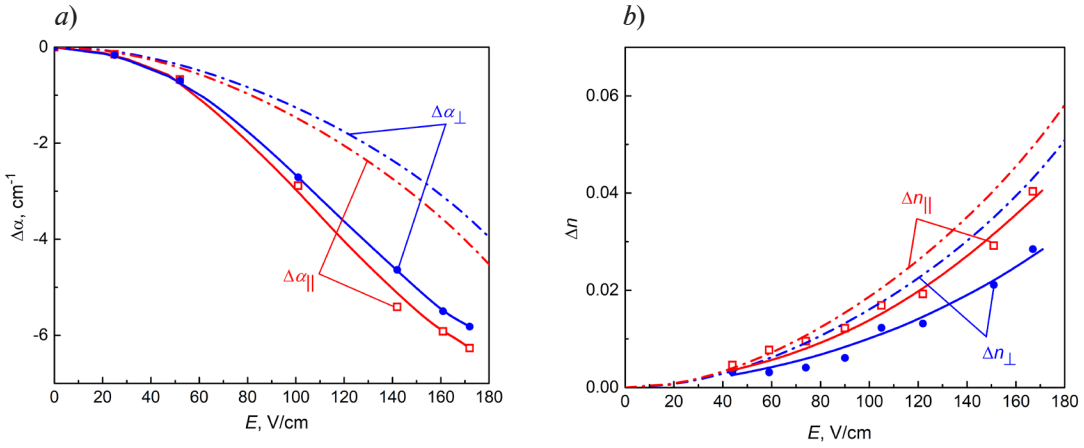

Fig. 4. Electric-field-induced change in the absorption coefficient of *n*-InSb, $\Delta\alpha_p(E)$, for radiation of two mutually orthogonal linear polarizations (P = ⊥, ∥) (*a*); circles and squares show the experimental values obtained from the transmittance modulation analysis in sample C, dash-dotted lines represent the results of theoretical modeling. Electric-field-induced change in the refractive index of *n*-InSb $\Delta n_p(E)$ for radiation of two linear polarizations (*b*); circles and squares show the experimental values obtained from the transmittance modulation analysis in sample PP, dash-dotted lines represent the simulation results.
Solid lines in both panels are a guide for the eye

The analysis of transmittance modulation in sample PP is, generally speaking, a more complex task. In this sample, due to multipath Fabry–Pérot interference, a significant contribution to the modulation comes from the change in the interference phase δ [see Eq. (1)], caused by the electric field-induced change in the refractive index $\Delta n_p(E)$, P = ⊥, ∥.

Let us write the nonequilibrium absorption coefficient for polarized light as $\alpha_p(E) = \alpha(0)+\Delta\alpha_p(E)$, and the nonequilibrium refractive index as $n_p(E) = n(0)+\Delta n_p(E)$, where α(0) and $n(0)$ are the equilibrium values of the absorption coefficient and refractive index ($E = 0$). Then, for a given polarization, using Eqs. (1) and (4), we can express the electric field-induced modulation M through α(0), $\Delta\alpha_p(E)$, $n(0)$ and $\Delta n_p(E)$. Since $\Delta\alpha_p(E)$ is already known from the experiment (Fig. 4, *a*), an analysis of the experimental field dependence of the transmittance modulation for this polarization allows us to find α(0), $n(0)$ and $\Delta n_p(E)$. We used the parameters α(0) and $n(0)$ as fitting parameters. Note that α(0) determines the contrast of the interference pattern, and $n(0)$ determines the number of the interference pattern period within which the phase δ changes under the effect of electric field.

When α(0) and $n(0)$ are specified, the magnitude of Δn_p can be uniquely found from the experimental modulation value. The optimal values of α(0) and $n(0)$ were found by an iterative procedure aimed at obtaining the value of $n(0)$ as close as possible to the model value of this parameter (the modeling procedure is described in the paper [4]). As a result of the analysis of the experimental field dependence of the transmittance modulation (Fig. 1), the dependences $\Delta n_p(E)$ (see Fig. 4, *b*) and the equilibrium optical parameters of *n*-InSb were found: $\alpha(0) = 19$ cm^{-1} (theoretical modeling gives a value of 26 cm^{-1}) and $n(0) = 3.975$ (theoretical modeling gives a value of 3.968). Accordingly, for sample PP in zero field the interference phase is $\delta \approx 41\cdot(2\pi)$, which corresponds to the 41st interference maximum. In a field of 167 V/cm $\Delta n_{\parallel}(E) = 0.040$ and $\Delta n_{\perp}(E) = 0.028$ (see Fig. 4, *b*), which corresponds to a significant increase in the interference phase (by 0.81π and 0.56π, respectively) and leads to a change in the modulation sign in Fig. 1, *a*. In this case, the refractive index anisotropy reaches a magnitude of $n_{\parallel}(E) - n_{\perp}(E) = 0.012$.

We also performed theoretical modeling of the dependences $\Delta\alpha_p(E)$ and $\Delta n_p(E)$ for two linear polarizations (P = ⊥, ∥). The calculation algorithm and the main calculation parameters were published in [4]. The calculation is based on a nonequilibrium stationary electron distribution function in the form of a shifted Fermi–Dirac distribution:

$$f(\mathbf{k}_c) = \frac{1}{\exp\left[\dfrac{\varepsilon(\mathbf{k}_c) - \hbar\mathbf{k}_c\mathbf{v}_{dr} - \varepsilon_F}{k_B T_e}\right] + 1}, \quad (6)$$

where $\mathbf{k}_c$ is the electron wave vector, $\varepsilon(\mathbf{k}_c)$ is the dispersion law for the conduction band, and k_B is the Boltzmann constant. The parameters of this function are the nonequilibrium electron temperature T_e, which exceeds the lattice temperature T_0, the electron drift velocity $\mathbf{v}_{dr}$, and the Fermi energy ε_F; all three parameters depend on the electric field E.

We determined the dependence $\mathbf{v}_{dr}(E) = -\mu(E)\mathbf{E}$ from the experimental current-voltage characteristic (CVC). Studies in pulsed operation mode showed that the dependences of the current density j on the field strength E for samples PP and C coincide within the experimental error (see Fig. 5, *a*). Over the entire range of electric fields, the CVC remains linear; therefore, $\mu(E) = \text{const} = \mu(0)$.

The temperature of nonequilibrium electrons T_e at a given electric field strength can be determined using the power balance equation:

$$q_e\mu(E)E^2 = \left\langle \frac{d\varepsilon}{dt} \right\rangle, \quad (7)$$

where q_e is the electron charge, and $\left\langle \dfrac{d\varepsilon}{dt} \right\rangle$ denotes the electron energy loss rate averaged over an ensemble of electrons with a given concentration. When calculating the energy loss rate, the scattering of electrons with optical phonons was considered, taking into account the electron-electron interaction [5]. The Coulomb logarithm required for the calculation was obtained on the basis of the work [6]. The dependence of the energy loss rate on the electron temperature, obtained at $N_e = 3.5 \cdot 10^{15}$ cm^{-3} and $T_0 = 78$ K, is shown in the inset to Fig. 5, *b*. Using this dependence, as well as the experimental data on $\mu(E)$, we determined the field dependence of the temperature of nonequilibrium electrons T_e (the algorithm of this procedure is described in detail in the paper [7]). The degree of heating of free electrons $\Delta T_e = T_e - T_0$ depending on the electric field is shown in Fig. 5, *b*. Under the conditions of our experiment, the field dependence of ΔT_e is close to quadratic (the relative deviation does not exceed 10%), which corresponds to a linear dependence on the supplied electric power. The maximum heating of electrons was 102 K (in a field of 180 V/cm).

The position of the Fermi level ε_F at the electron temperature T_e was determined by normalizing the distribution function (6) to the electron concentration N_e.

A comparison of the results of theoretical modeling of the dependences $\Delta\alpha_p(E)$ and $\Delta n_p(E)$ for two linear polarizations with the experimental results is shown in Fig. 4 *a*, *b*. The model

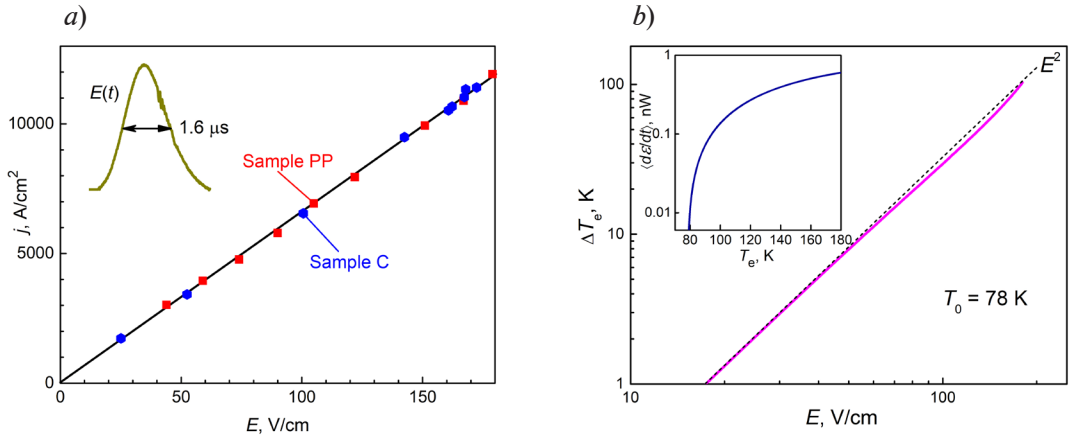

Fig. 5. Experimental current–voltage characteristics for two samples (*a*), inset: electric field pulse shape. Field dependence of electron temperature (*b*), obtained from the current–voltage characteristics using the power balance equation, inset: energy loss rate per electron vs. the nonequilibrium electron temperature T_e (theoretical simulation)

field dependences are in qualitative agreement with the experimental ones: (*i*) the absorption coefficients for both polarizations decrease with the field, (*ii*) the anisotropy $\alpha_{\parallel} - \alpha_{\perp}$ is negative and increases in absolute value with increasing field, (*iii*) the refractive indices for both polarizations increase with field, (*iv*) the anisotropy $n_{\parallel} - n_{\perp}$ is positive and increases with increasing field.

A quantitative comparison shows that the model calculation yields an anisotropy of the absorption coefficient $\alpha_{\parallel}(E) - \alpha_{\perp}(E)$ that coincides with the experiment with an accuracy of 10%, while the simulation yields a weaker average decrease in the absorption coefficient $[\alpha_{\parallel}(E) + \alpha_{\perp}(E)]/2$ in strong fields compared to the experiment (by approximately 40%).

The simulated anisotropy of the refraction coefficient $n_{\parallel}(E) - n_{\perp}(E)$ is approximately two times smaller than that observed in the experiment, while the simulation yields a stronger average increase in the refractive index $[n_{\parallel}(E) + n_{\perp}(E)]/2$ in strong fields compared to the experiment (by approximately 30%).

This quantitative difference between the experimental and theoretical modeling results may be due in part to experimental imperfections and in part to the approximate nature of the model. Specifically, the experiment utilized bell-shaped electric field pulses with a duration comparable to the photodetector time constant, and no correction for the photodetector's dynamic error was made when analyzing the photoresponse waveform. Theoretical calculations of the change in the absorption coefficient and refractive index of *n*-InSb in an electric field were based on a model dependence of the energy loss rate $\left\langle \frac{d\varepsilon}{dt} \right\rangle$ on the electron temperature, obtained without taking into account non-parabolicity of the conduction band.

Summary

Electric-field-induced changes in the absorption coefficient and refractive index for terahertz radiation in *n*-InSb were experimentally detected and studied. The studies were conducted in the pre-breakdown electric field region (less than 180 V/cm), where the free electron concentration remains constant. Polarization anisotropy of both effects was revealed. The current-voltage characteristics of the samples used for electro-optical studies were also measured. In the studied electric field region, the current-voltage characteristics are linear. It was found that the maximum electron heating reached ~100 K, and the maximum drift velocity was approximately $2.2 \cdot 10^7$ cm/s.

Theoretical modeling of the studied effects was performed. It was shown that they are caused by the combined effect of the non-parabolicity of the indium antimonide conduction band and the anisotropy of the electron distribution function over states in momentum space, associated with electron heating and drift.

The research results can be used in the development of high-speed modulators of terahertz radiation.

Acknowledgments

The work was supported by the Russian Science Foundation (grant № 23-12-00036).

REFERENCES

1. **Ma Z.T., Geng Z.X., Fan Z.Y., Liu J., Chen H.D.,** Modulators for Terahertz Communication: The Current State of the Art, Research. 2019 (2019) 6482975.

2. **Huang Y., Shen Y., Wang J.,** From terahertz imaging to terahertz wireless communications, Engineering. 22 (2023) 106–124.

3. **Vorobjev L.E., Stafeev V.I., Firsov D.A.,** Influence of heating and drift of electrons on the refractive index of *n*-type InSb determined allowing for band-band transitions, Soviet Physics: Semiconductors. 18 (3) (1984) 317–320.

4. **Karaulov D.A., Vinnichenko M.Ya., Shalygin V.A., Firsov D.A.,** The effect of electron heating and drift in an electric field on the absorption and refraction of terahertz radiation in *n*-InSb, St. Petersburg State Polytechnical University Journal. Physics and Mathematics. 18 (4) (2025) (to be published).

5. **Gelmont V.L., Lyagushchenko R.I., Yassievich I.N.,** Distribution function and energy loss of hot electrons under interaction with optical phonons, Fizika tverdogo tela. 14 (2) (1972) 533 (in Russian).
6. **Kramers H.A.,** The stopping power of a metal for alpha-particles, Physica. 13 (6-7) (1947) 401.
7. **Shalygin V.A., Makhov I.S., Adamov R.B., Vinnichenko M.Ya., Khvostikov V.P., Firsov D.A.,** Electric-field-induced polarization anisotropy of interband photoluminescence in GaAs, Journal of Applied Physics. 136 (19) (2024) 195703.

THE AUTHORS

USTIMENKO Ratmir V.
ratmirustimenko@yandex.ru
ORCID: 0000-0003-4123-4375

MELENTEV Grigorii A.
gamelen@spbstu.ru
ORCID: 0000-0002-1680-333X

SHALYGIN Vadim A.
vadim_shalygin@mail.ru
ORCID: 0000-0001-6728-7286

VINNICHENKO Maxim Ya.
mvin@spbstu.ru
ORCID: 0000-0002-6118-0098

KARAULOV Danila A.
donil793@yandex.ru
ORCID: 0009-0002-1608-3659

FIRSOV Dmitry A.
dmfir@rphf.spbstu.ru
ORCID: 0000-0003-3947-4994

NORVATOV Ilya A.
norv2@mail.ru
ORCID: 0000-0002-0048-7514

Received 17.11.2025. Approved after reviewing 24.11.2025. Accepted 03.12.2025.